# X-ray energy dispersive spectroscopy of uranium ore using a TES microcalorimeter mounted on a field-emission scanning electron microscope

Maehata, Keisuke
Department of Applied Quantum Physics and Nuclear Engineering, Kyushu University

Idemitsu, Kazuya
Department of Applied Quantum Physics and Nuclear Engineering, Kyushu University

Tanaka, Keiichi
SII Nano Technology Inc.



出版情報：Nuclear Instruments and Methods in Physics Research, Section A : Accelerators, Spectrometers, Detectors and Associated Equipment. 648 (1), pp.285-289, 2011-08-21. Elsevier
バージョン：

# X-ray Energy Dispersive Spectroscopy of Uranium Ore using a TES Microcalorimeter Mounted on a Field-Emission Scanning Electron Microscope

Keisuke Maehata[a,*], Kazutya Idemitsu[a], Keiichi Tanaka[b]

[a] *Department of Applied Quantum Physics and Nuclear Engineering, Kyushu University, 744 Motooka, Nishi-ku, Fukuoka-shi, 819-0395, JAPAN*
[b] *SII NanoTechnology Inc., 36-1 Takenoshita, Oyama, Sunto, Shizuoka 410-1393, JAPAN*

**Abstract**

Energy dispersive spectroscopic measurements of uranium-ore were conducted using a superconducting phase transition-edge-thermosensor (TES) microcalorimeter mounted on a field-emission scanning electron microscope (SEM) to demonstrate its potential for high-precision microanalysis. The effective solid angle for X-ray detection is found to be larger than 2msr by precise adjustments in the X-ray polycapillary alignment. The observed detection signal pulses with decay time constant of 50 $\mu$s enable maximum count rates larger than 300 counts per second. The energy resolution was determined to be 14.6 eV FWHM at Al $K_\alpha$ X-ray energies of 1487 eV. Distinct peaks appear in the resulting X-ray energy spectrum associated with U-$M_\alpha$, U-$M_\beta$ and U-$M_\gamma$ X-rays emitted by the uranium-ore specimens. This spectrum includes weaker peaks corresponding to C-$K_\alpha$, Fe-$L_\alpha$, Cu-L and Sr $L_{\alpha 1}$ X rays.

*Keywords:*
TES microcalorimeter, Energy dispersive spectroscopy, Scanning electron microscope, X-ray microanalysis, Compact dilution refrigerator

## 1. Introduction

A scanning electron microscope (SEM) is a tool used to obtain micro- or nano-scale images of specimens required in research and development of materials, electronic devices, and the like. Specimens in the SEM are irradiated with a

*Corresponding author. Tel: +81 92 802 3481; fax: +81 92 802 3483.
*Email address:* maehata@nucl.kyushu-u.ac.jp (Keisuke Maehata)

finely focused electron beam of diameter $\sim 10^{-9}$ m and emit secondary electrons from the their irradiated surfaces. The SEM images are formed by analyzing the intensity of these emitted secondary electrons as a function of irradiated position on the specimen. The emitted secondary electrons induce characteristic X-ray emissions from elements contained in the specimen. Spectroscopic measurements of these characteristic X-rays enable an analysis of the composition of elements from a very small local structure area within the specimen. The precision of that analysis strongly depends on the energy resolution of the X-ray detection.

Usually, spectroscopic measurements of the characteristic X-rays are conducted by means of two types of spectroscopy, wavelength-dispersive spectroscopy (WDS) and energy-dispersive spectroscopy (EDS). Excellent energy resolution, typically $2-20$ eV, has been achieved in WDS. However, WDS has several disadvantages such as low detection efficiency, narrow energy range, and errors caused by misalignment in the measurement system. EDS allows quantitative analysis with a rather simple operation compared with WDS. Si(Li) semiconductor detectors are used in the detection of X-rays in typical EDS systems. Accuracy though is limited also by the energy resolution of the X-ray detectors. The energy resolution of Si(Li) semiconductor detectors has achieved their theoretical limit of 120 eV full width at half maximum (FWHM) value of 5.9 keV. Therefore, the development of an X-ray detector with excellent energy resolution is necessary for EDS performed with the SEM.

Several types of superconducting phase transition edge thermosensor (TES) microcalorimeters have been developed that operate with excellent energy resolution of better than 10 eV FWHM value in X-ray detection [1]. Energy resolutions have improved to FWHM values of 1.8 eV at 5.9 keV[2]. The TES microcalorimeter has been utilized in X-ray detectors for EDS performed with SEM. Irwin *et al.* attached a TES microcalorimeter to a SEM and detected the Ti $K_\alpha$ line (4.5 keV) with FWHM of 13.9 eV[3]. D. A. Wollman *et al.* developed a TES microcalorimeter EDS system mounted on a SEM[4].

In this work, EDS measurements of uranium-ore were conducted by a SEM-

mounted TES microcalorimeter system to demonstrate the potential for high-precision microanalysis.

## 2. TES microcalorimeter EDS system mounted on SEM

Fig. 1 shows a photograph of a TES-EDS system mounted on a field-emission SEM (Carl Zeiss SUPRA 40) manufactured by SII NanoTechnology Inc. A TES microcalorimeter chip is glued on the top of the snout extending from a mixing chamber of a compact $^3$He-$^4$He dilution refrigerator (DR). The snout is inserted into the vacuum chamber of the SEM through an X-ray detector port. The bottom of the DR is tightly fixed on a position-adjustment system attached to a flange of an SEM port. Fig. 2 shows a photograph of the refrigeration system which includes the DR, a liquid helium vessel, a liquid helium transfer tube, and a full-automatic gas handling system.

A schematic diagram of the refrigeration system is illustrated in Fig. 3. Liquid helium is transferred to the DR through the flexible transfer tube by exhausting evaporated helium gas at the gas outlet of the transfer tube. The temperature of liquid helium is reduced to 2.5 K through the impedance $Z_{He}$ at the liquid outlet of the transfer tube. Cold liquid helium returns to the transfer tube through heat exchangers HX3, HX2, and HX1 to condense the gaseous $^3$He-$^4$He mixture at a temperature of 2.5 K. After being sufficiently precooled by heat exchangers HX1 and HX2, the gaseous $^3$He-$^4$He mixture is condensed through the heat exchanger HX3 and flows into the concentrated $^3$He mixture. This mixture flows into heat exchanger HX4 in the still through the impedance Z and then enters heat exchanger HX5. Here, the concentrated $^3$He mixture flows through the capillary coiled around a plunger and is cooled by the dilute $^3$He mixture flowing in the channel between the inner surface of the sheath and the outer surface of the coiled capillary. After being cooled in HX5, the concentrated $^3$He mixture enters the mixing chamber 1 (MC1) of a cascade of two mixing chambers. A portion of the $^3$He mixture flow is diluted in MC1 and returned to the dilute flow channel in the heat exchanger through the flow

impedance $Z_{MC}$. The rest of the mixture is precooled to the temperature of the mixing chamber 2 (labeled MC2) through the heat exchanger HX6 which has similar structure to HX5. In MC2, the inflowing concentrated $^3$He mixture is diluted and returned to the still through HX6 and HX5. This gas mixture is pumped out of the still and allowed to flow towards the circulation pump through heat exchangers. The snout rod is extended from a base-block attached to the base plate of MC2. The flow-rate of the gaseous $^3$He-$^4$He mixture is controlled by a fully-automatic gas handling system. The temperature at the top of the snout is maintained at a TES microcalorimeter operation temperature within a range of 10 $\mu$K. The consumption rate of liquid helium is 40 $l$/day in the TES microcalorimeter operation.

The TES microcalorimeter consists of a thin-film thermometer with a bilayer structure of Au/Ti and an absorbing Au layer deposited on the thermometer film. The area of the absorber is 200 $\mu$m $\times$ 200 $\mu$m. The Au absorber of 0.5 $\mu$m thickness allows the TES microcalorimeter to detect X-ray photons with energy of 300 eV to 6 keV emitted by a sample in the SEM with an absorption efficiency above 50%. The electric current through the TES decreases with rising temperature caused by a deposition of X-ray energy in the absorber. A change in the current is converted into a voltage signal by a superconducting quantum interference device (SQUID) amplifier. A collimator was assembled in front of the absorber. An X-ray polycapillary is placed between the TES microcalorimeter and the specimen. The effective solid angle is found to be larger than 2msr by a precise adjustment of the X-ray polycapillary alignment. In preliminary test operations, the phase transition temperature of the TES was observed to be 200 mK. Fig. 4 shows an example of the output voltage signal pulse of the SQUID amplifier obtained during X-ray detection. The maximum count rate is estimated to be higher than 300 cps by using an observed pulse decay time constant of 50 $\mu$s. As shown in Fig. 5, the energy resolution was found to be 14.6 eV FWHM at Al $K_\alpha$ X ray of 1487 eV.

## 3. Energy dispersive x-ray spectroscopy of uranium-ore

In this work, uranium-ore was selected to demonstrate the potential for a microanalysis using an SEM-mounted TES-EDS system. Fig. 6 shows a typical SEM image of a uranium-ore specimen. EDS was performed under electron beam irradiation in the area indicated by a rectangle in Fig. 6. The electron beam was accelerated with an applied voltage of 7 kV. Detection signal pulses were accumulated during 600 seconds of irradiation. Fig. 7 shows the energy spectrum of the characteristic X-rays obtained from the EDS measurements. Distinct peaks in the energy spectrum correspond to U-$M_\alpha$ X-rays of energy 3171 eV, U-$M_\beta$ X-rays of 3337 eV, P-$K_\alpha$ X-rays of 2014 eV, Si-$K_\alpha$ X-rays of 1740 eV, Al-$K_\alpha$ X-rays of 1487 eV, and O-$K_\alpha$ X-rays of 525 eV, as labeled in Fig.7. Fig. 8 shows details of the X-ray energy spectrum over the energy range from 3000 to 4000 eV. Here the peaks in the energy spectrum correspond to U-$M_\alpha$ X-rays of 3171 eV, and U-$M_\beta$ X-ray of 3337 eV, U-$M_\gamma$ X-ray of 3565 eV, and Ca-$K_\alpha$ X-ray of 3692 eV, as labeled in Fig. 8. Details of the X-ray energy spectrum in the energy range from 1500 to 2000 eV is shown in Fig. 9. For comparison, the dashed line in Fig. 9 indicates results of EDS measurements for a W specimen. Peaks corresponding to Si-$K_\alpha$ X-rays of 1740 eV and W-$M_{\alpha 1}$ X-rays of 1775 eV are clearly identified in the X-ray energy spectrum. The small peak at 1807 eV corresponding to Sr-$L_{\alpha 1}$ X-rays between the W-M X-ray peaks represents an improvement in the effective detection limit of conventional EDS measurement. Fig. 10 shows the X-ray spectrum in the low energy region. Small peaks are identifiable; these correspond to C-$K_\alpha$ X-rays of 277 eV, Fe-$L_\alpha$ X-rays of 705 eV, and Cu-L X-ray of 930 eV, as labeled in Fig. 10.

## 4. Conclusions

EDS measurements of uranium-ore were conducted using a TES microcalorimeter system mounted on a SEM. The energy resolution attained was 14.6 eV FWHM at Al $K_\alpha$ X ray of 1487 eV. Distinct peaks associated with U-$M_\alpha$, U-$M_\beta$, and U-$M_\gamma$ X-rays appeared in the energy spectrum resulting from X-rays

emitted by a specimen of the uranium-ore. The obtained energy spectrum included weaker peaks corresponding to C-$K_\alpha$, Fe-$L_\alpha$, Cu-L and Sr $L_{\alpha 1}$ X rays. The obtained energy spectrum showed the SEM-mounted TES-EDS system has the potential for high-precision microanalysis.

## References


[1] G. Angloher, Nucl. Instru. and Meth., A512 (2003) 401-407.

[2] S. R. Bandler,R. P. Brekosky, A. -D. Brown, J. A. Chervenak, E. Figueroa-Feliciano, F. M. Finkbeiner, N .Iyomoto, R. L. Kelley, C. A. Kilbourne, F. S. Porter, J. Sadleir and S. J. Smith, J. Low Temp. Phys., 151 (2008) 400-405.

[3] K. D. Irwin, G. C. Hilton, D. A. Wollman and John M. Martinis, Appl. Phys. Lett., 69 (1996) 1945-1947.

[4] D. A. Wollman, S. W. Nam, D. E. Newbury, G. C. Hilton, K. D. Irwin, N. F. Bergren, S. Deiker, D. A. Rudman and J. M. Martinis, Nucl. Instru. and Meth., A444 (2000) 145-150.

**Figure Captions**

Fig. 1 Photograph of the TES-EDS system mounted on a field-emission SEM (Carl Zeiss SUPRA 40) manufactured by SII NanoTechnology Inc.

Fig. 2 Photograph of the refrigeration system composed of the dilution refrigerator (DR), a liquid helium vessel, a liquid helium transfer tube and a full-automatic gas handling system.

Fig. 3 Schematic of the refrigeration system for the TES microcalorimeter.

Fig. 4 Typical output voltage of a signal pulse from the SQUID amplifier in X-ray detections.

Fig. 5 Energy spectrum of the Al $K_\alpha$ X-rays obtained with the SEM-mounted TES-EDS system.

Fig. 6 A SEM image of the uranium-ore specimen.

Fig. 7 Energy spectrum of the characteristic X-rays for uranium ore obtained from EDS measurements performed with the SEM-mounted TES microcalorimeter system.

Fig. 8 Detail from Fig.7 of the UM X-ray spectrum.

Fig. 9 Detail from Fig.7 of the energy spectrum in energy range $1500-2000$ eV.

Fig. 10 Detail from Fig.7 of the energy spectrum in energy range $0-1000$ eV.

Figure1

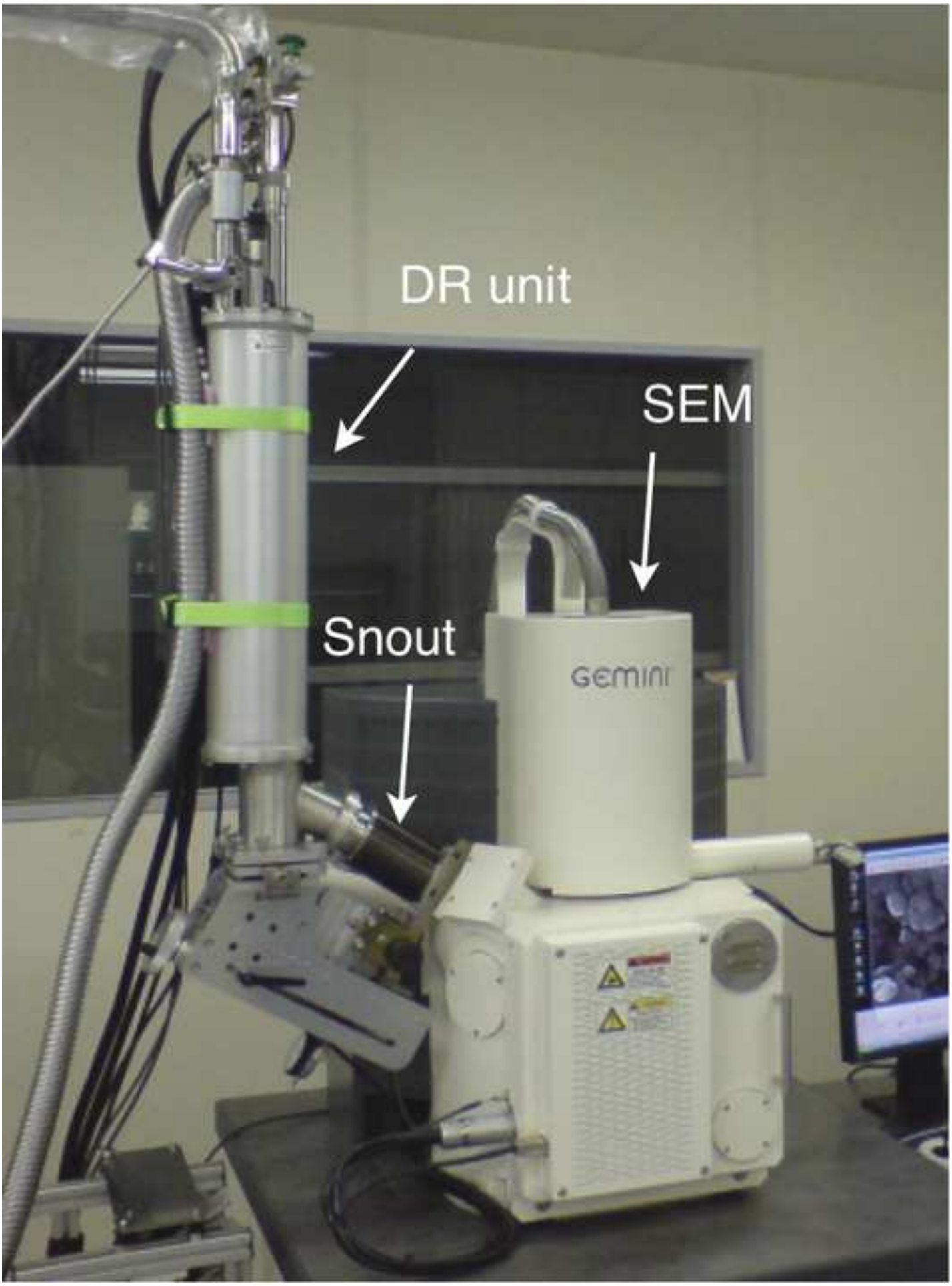

Figure2

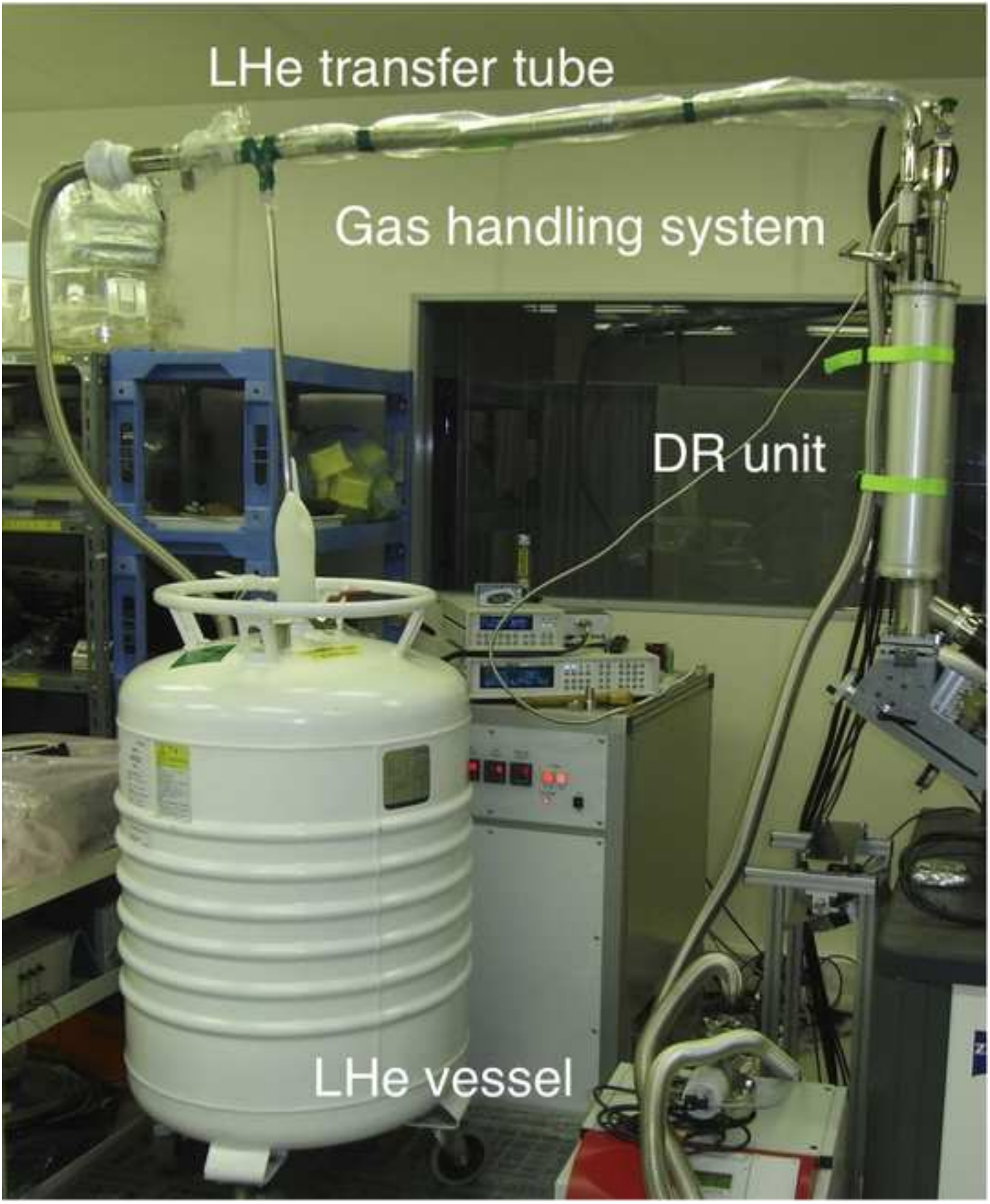

Figure3

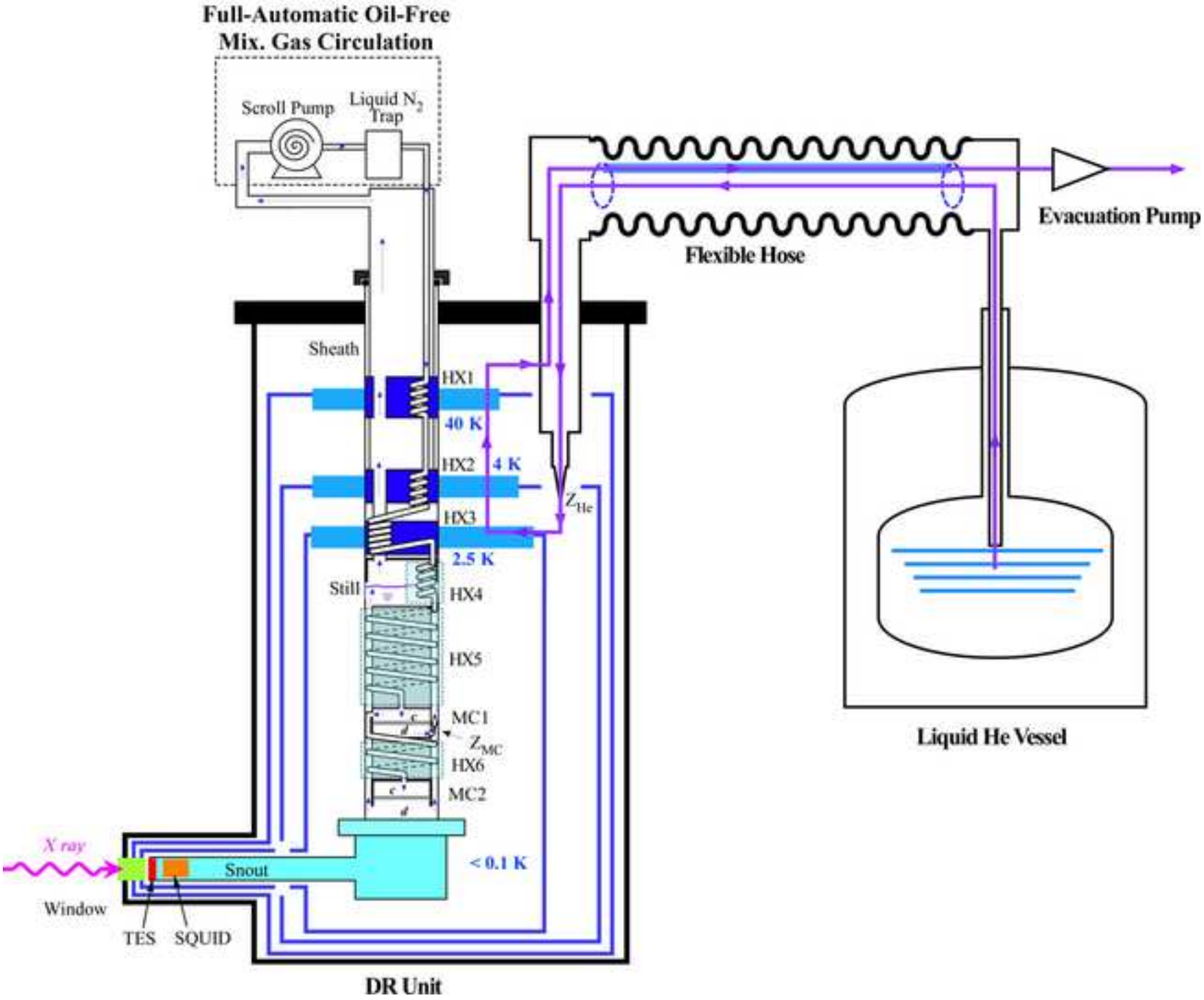
Full-Automatic Oil-Free
Mix. Gas Circulation
Scroll Pump
Liquid $N_2$ Trap
Evacuation Pump
Flexible Hose
Sheath
HX1
40 K
HX2
4 K
HX3
$Z_{He}$
2.5 K
Still
HX4
HX5
MC1
$Z_{MC}$
HX6
MC2
< 0.1 K
X ray
Snout
Window
TES
SQUID
Liquid He Vessel
DR Unit

Figure4

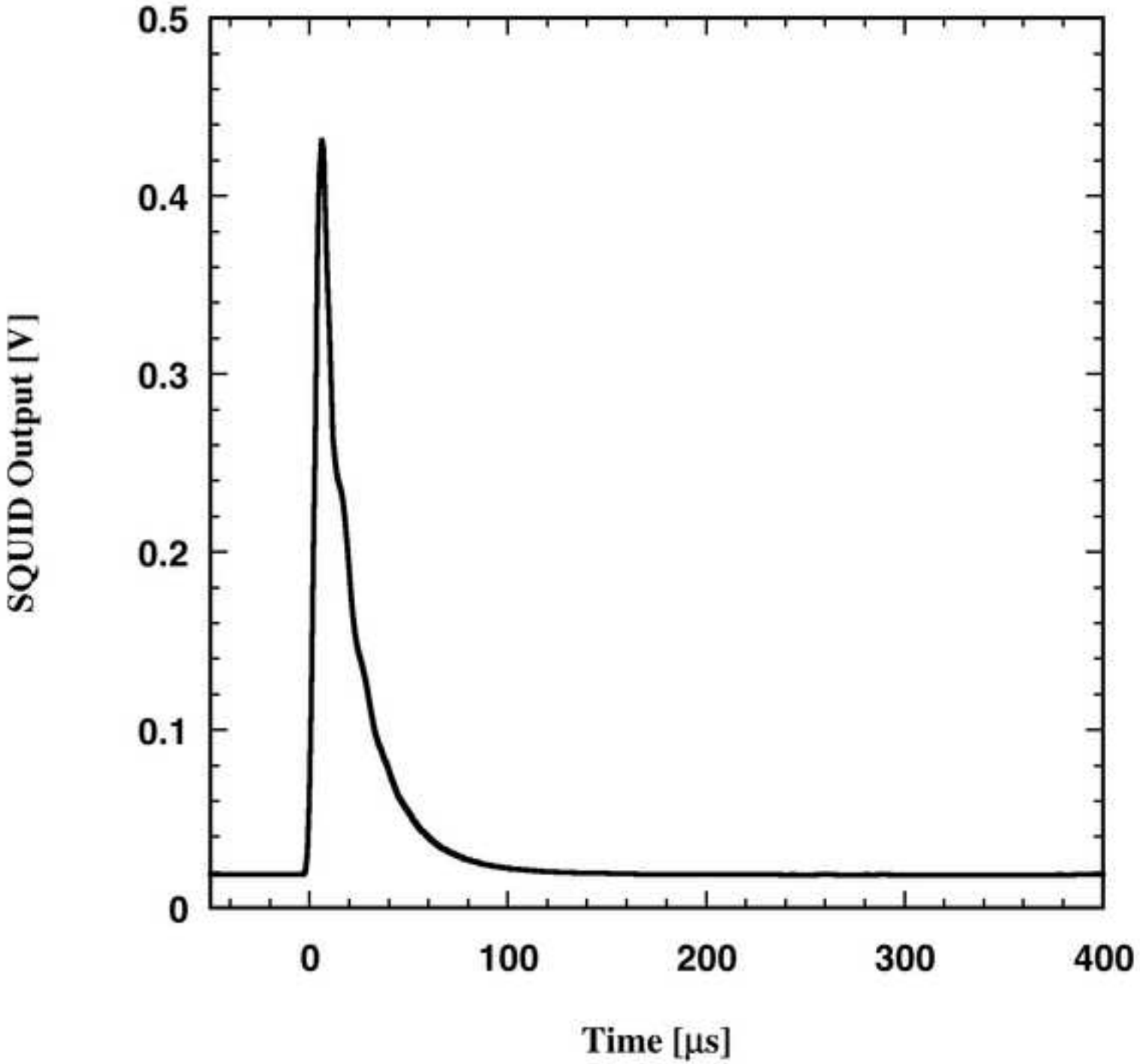

Figure5

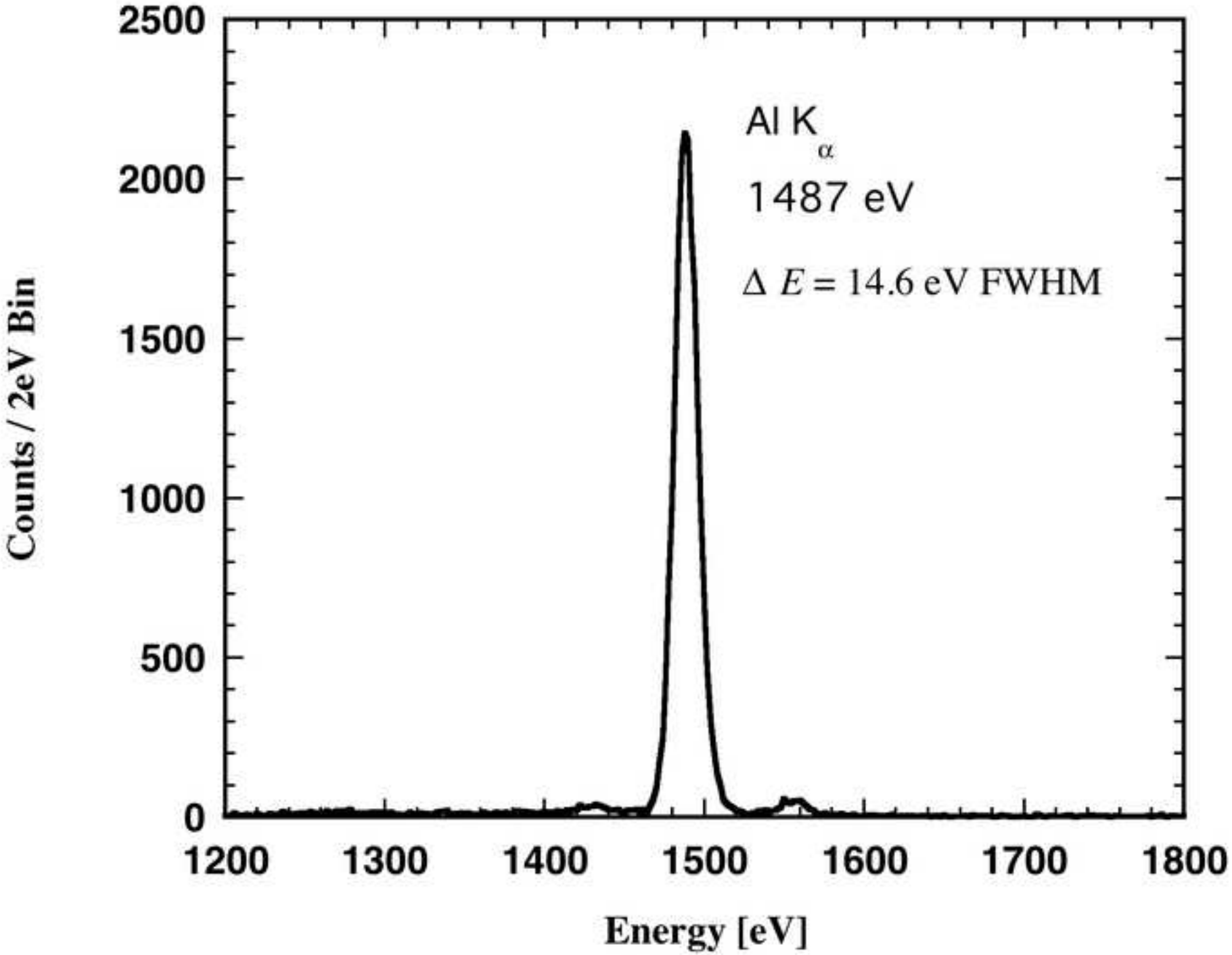
Al K
α
1487 eV
Δ E = 14.6 eV FWHM
Counts / 2eV Bin
Energy [eV]
0
500
1000
1500
2000
2500
1200
1300
1400
1500
1600
1700
1800

Figure6

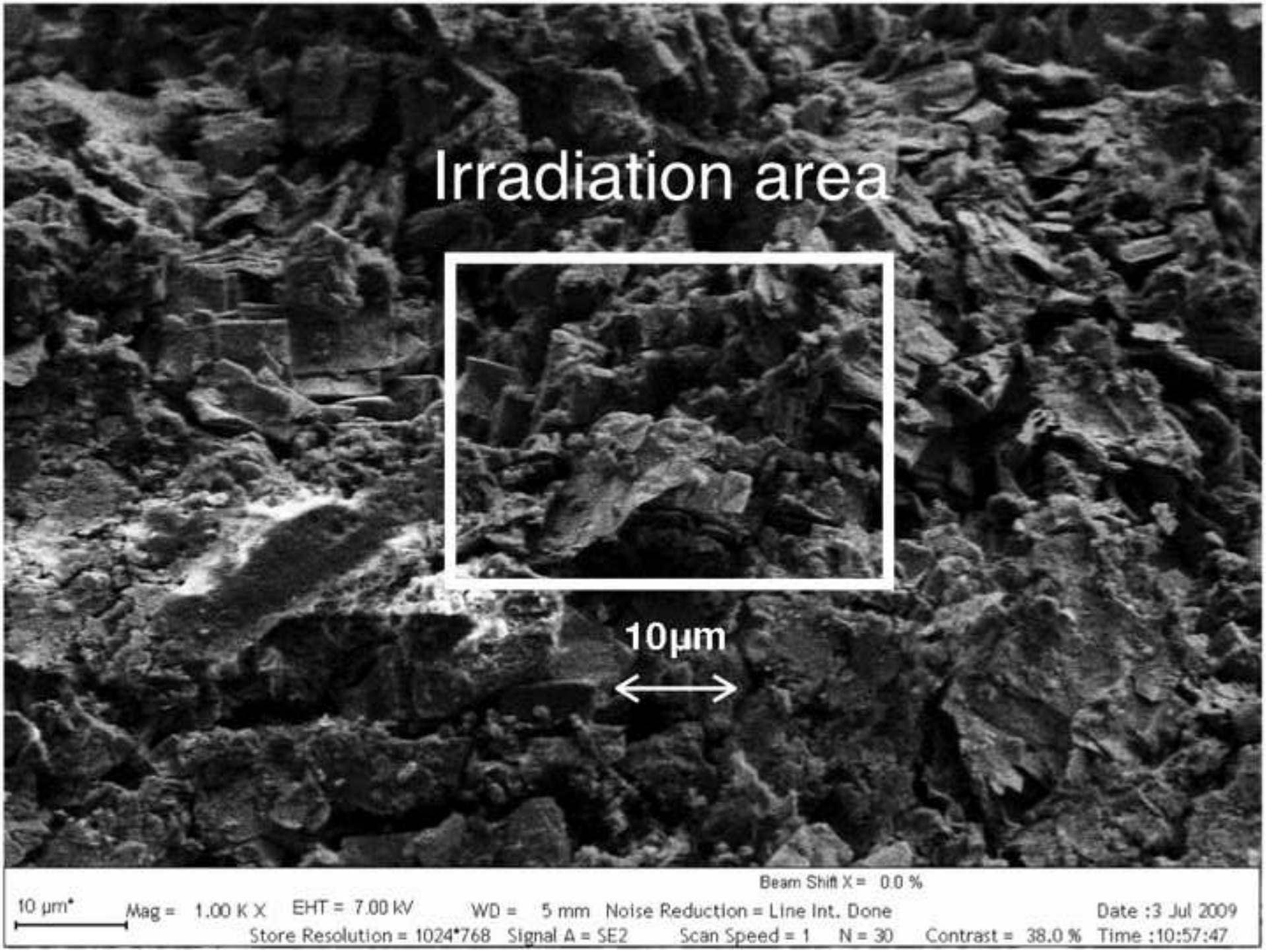
Irradiation area
10μm
Beam Shift X = 0.0 %
10 μm*
Mag = 1.00 K X
EHT = 7.00 kV
WD = 5 mm
Noise Reduction = Line Int. Done
Date :3 Jul 2009
Store Resolution = 1024*768
Signal A = SE2
Scan Speed = 1
N = 30
Contrast = 38.0 %
Time :10:57:47

Figure7

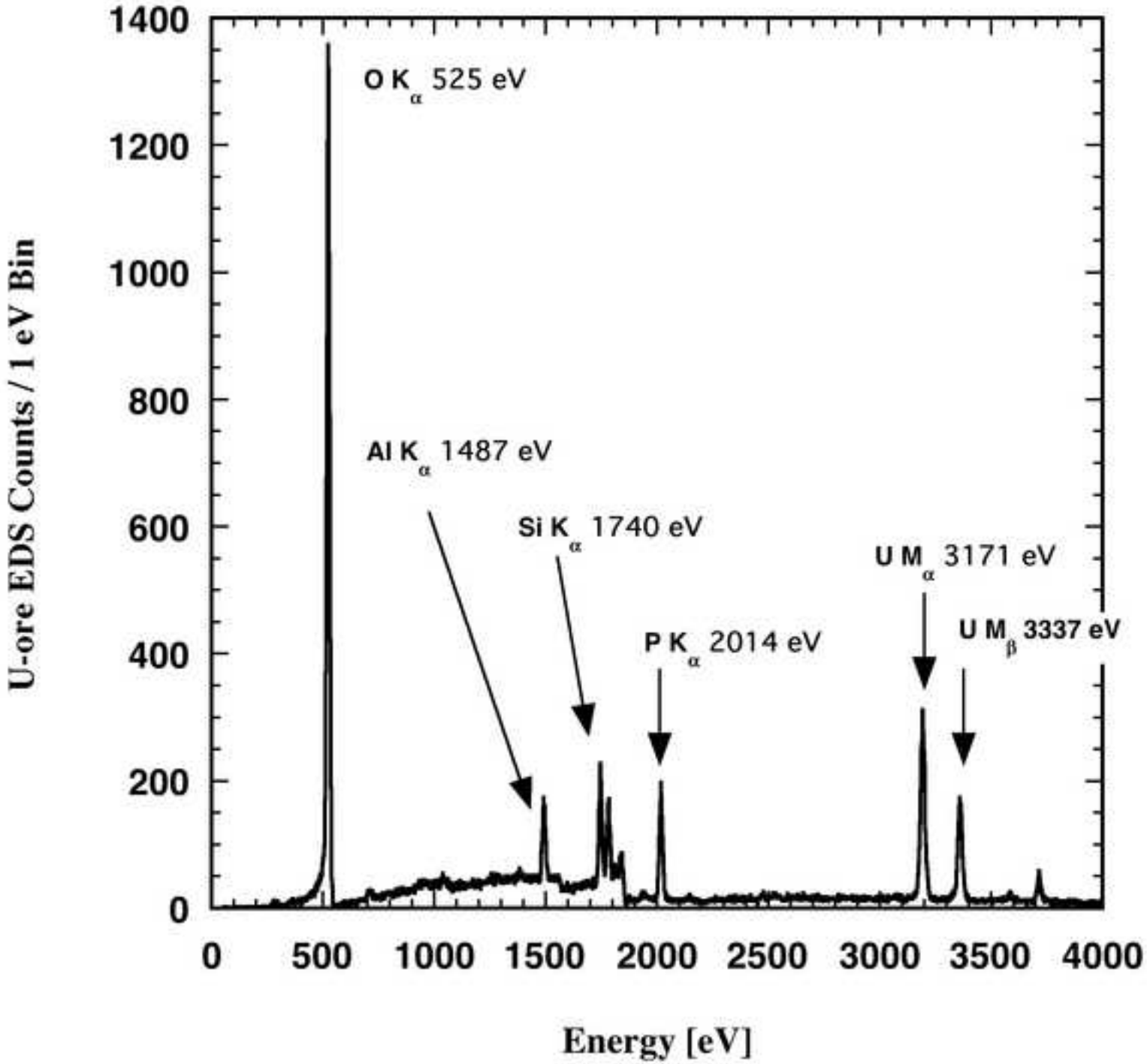
1400
1200
1000
800
600
400
200
0
0
500
1000
1500
2000
2500
3000
3500
4000
U-ore EDS Counts / 1 eV Bin
Energy [eV]
O Kα 525 eV
Al Kα 1487 eV
Si Kα 1740 eV
P Kα 2014 eV
U Mα 3171 eV
U Mβ 3337 eV

Figure8

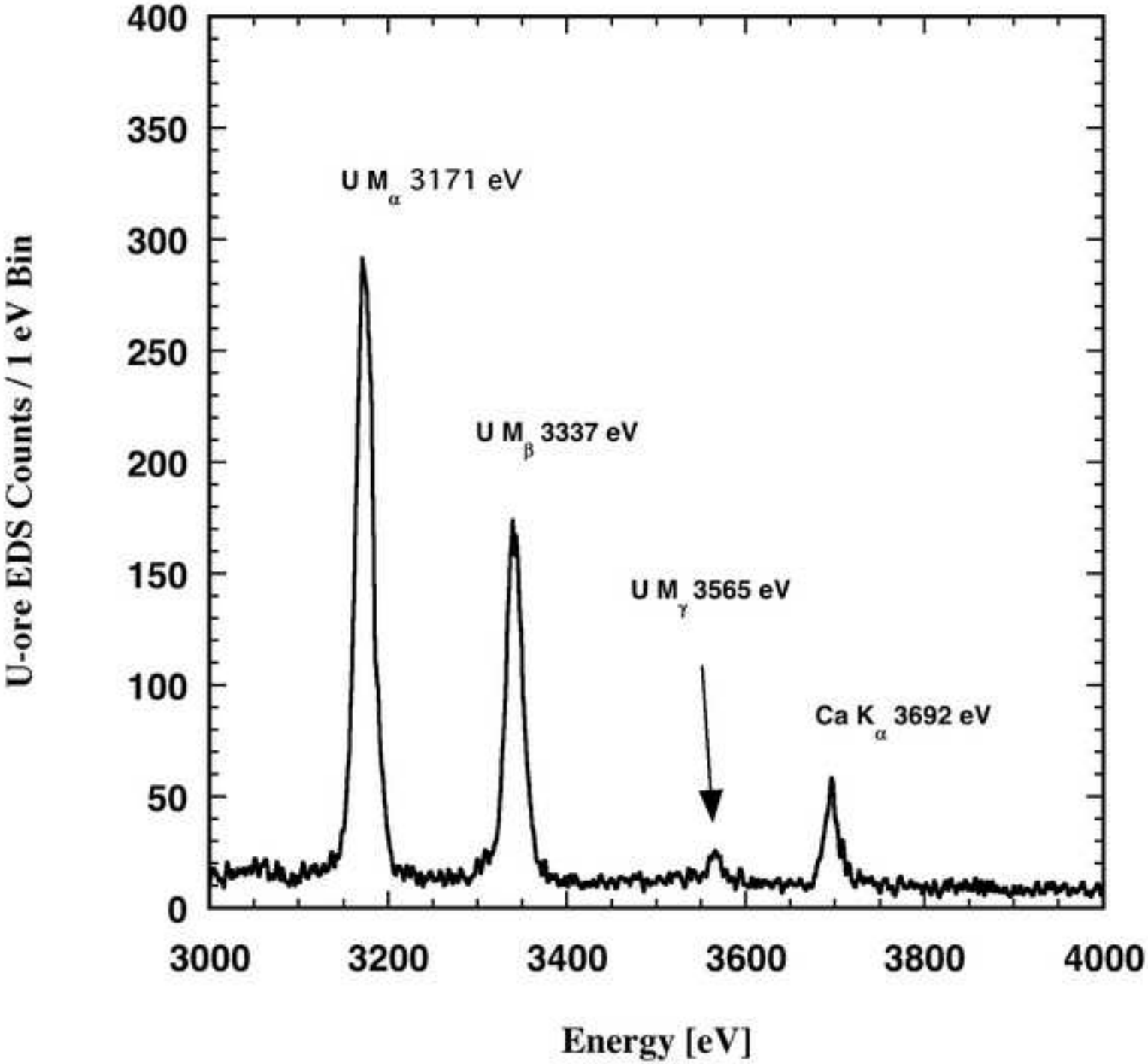
U-ore EDS Counts / 1 eV Bin
Energy [eV]
U M$_\alpha$ 3171 eV
U M$_\beta$ 3337 eV
U M$_\gamma$ 3565 eV
Ca K$_\alpha$ 3692 eV
0
50
100
150
200
250
300
350
400
3000
3200
3400
3600
3800
4000

Figure9

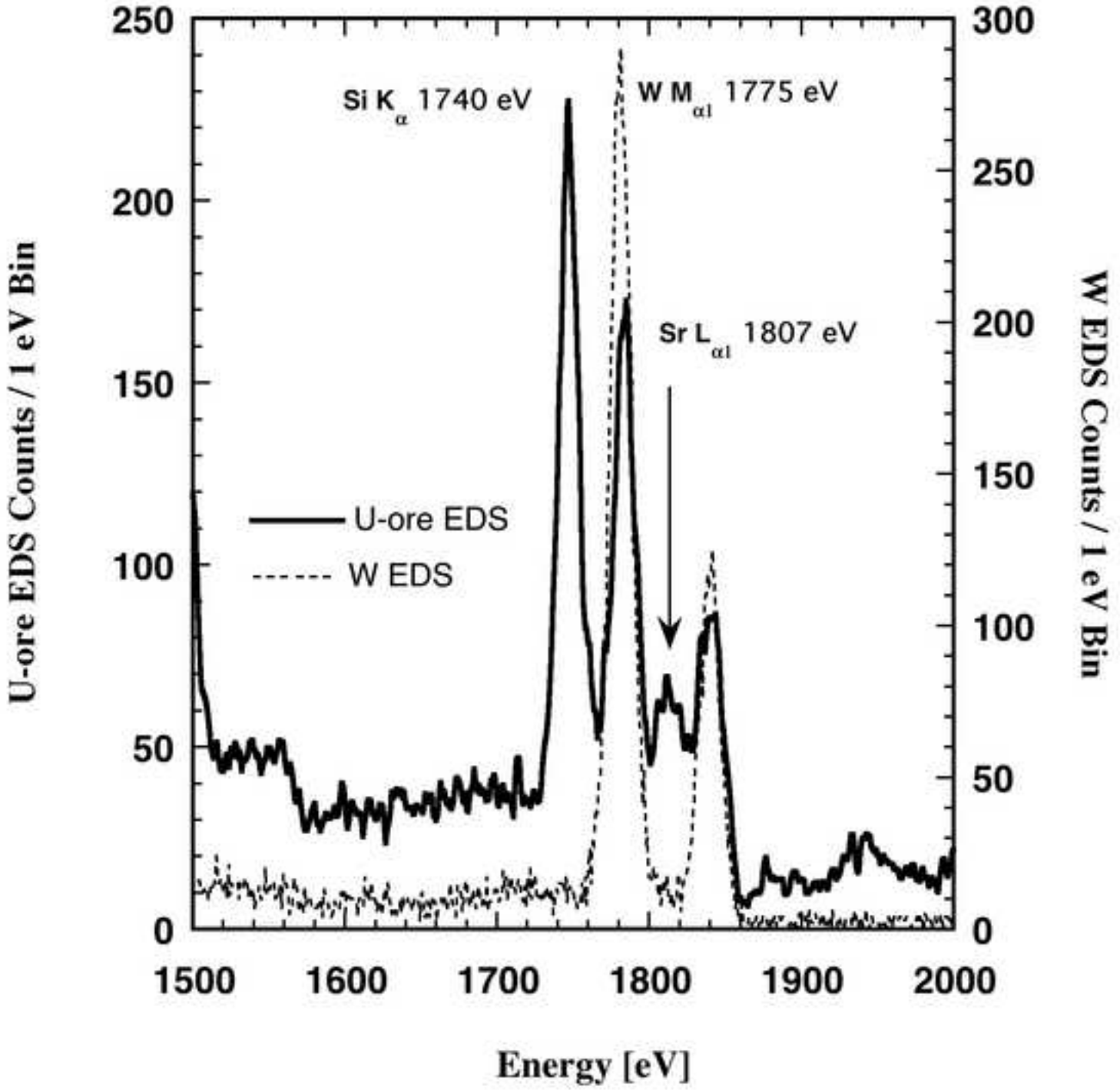
Si K$_\alpha$ 1740 eV
W M$_{\alpha 1}$ 1775 eV
Sr L$_{\alpha 1}$ 1807 eV
U-ore EDS
W EDS
U-ore EDS Counts / 1 eV Bin
W EDS Counts / 1 eV Bin
Energy [eV]
0
50
100
150
200
250
300
1500
1600
1700
1800
1900
2000

Figure10

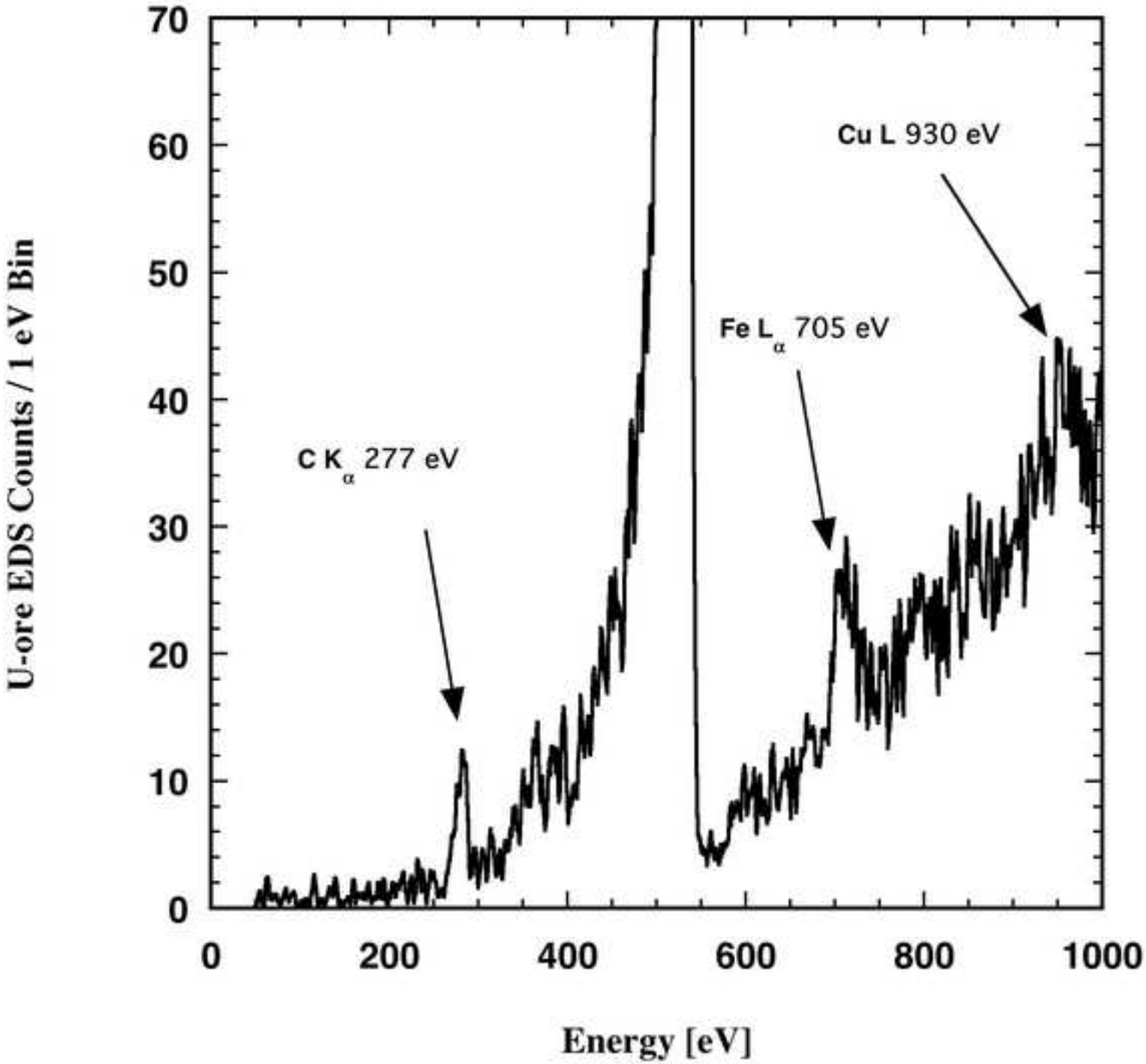
U-ore EDS Counts / 1 eV Bin
Energy [eV]
C K$_\alpha$ 277 eV
Fe L$_\alpha$ 705 eV
Cu L 930 eV
0
10
20
30
40
50
60
70
0
200
400
600
800
1000